Mathematical Modelling and Control

https://www.aimspress.com/journal/mmc

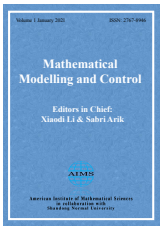

MMC, 5(3): 305–320.
DOI: 10.3934/mmc.2025021
Received: 23 January 2025
Revised: 01 April 2025
Accepted: 24 May 2025
Published: 13 August 2025

Research article

Complex dynamics for a discretized fractional-order predator-prey system with constant-yield prey harvesting and fear effect

Dengfeng Wang, Xianyi Li*, Xiao Zhu and Enrui Zhang

Department of Big Data Science, School of Science, Zhejiang University of Science and Technology, Hangzhou 310023, China

* **Correspondence:** Email: mathxyli@zust.edu.cn.

Abstract: In this paper, we derived and studied the discrete version of a continuous fractional-order predator-prey system with constant-yield prey harvest and a monotonically increasing function response, as well as a fear effect of the predator on the bait. After studying in detail the existence and local stability of the fixed points of the system, some favorable conditions for the occurrence of its Neimark–Sacker bifurcation and period-doubling bifurcation were obtained by using the central manifold theorem and bifurcation theory. Finally, numerical simulations carried out using Matlab software illustrate the theoretical results previously obtained and reveal its some new dynamics–the chaotic occurrence.

Keywords: Caputo fractional derivative; discrete predator-prey system; Neimark–Sacker bifurcation; period-doubling bifurcation

Mathematics Subject Classification: 39A28, 39A30

1. Introduction

With the continuous development of human society and civilization progress, resource consumption and environmental pollution have steadily increased. These present significant consequences, including frequent natural disasters and widespread viral outbreaks. Consequently, it is increasingly critical to look for strategies to address these environmental challenges. Mathematical modeling serves as a powerful tool in understanding and predicting the natural phenomena, offering valuable insights into ecological stability. As a result, there is a growing interest among researchers in employing mathematical approaches to study and resolve issues related to ecological balance.

Generally speaking, the classical predator-prey model has the following structure:

$$\begin{cases} \dfrac{dx}{dt} = f(x)x - g(x,y)y, \\ \dfrac{dy}{dt} = \epsilon g(x,y)y - \mu y, \end{cases} \tag{1.1}$$

where $x(t)$ and $y(t)$ represent the population densities of prey and predator in time t, respectively, $f(x)$ is the net growth rate of prey without predator, $g(x,y)$ is the consumption rate of prey by the predator, ϵ and μ are the positive constants respectively representing the conversion rate of captured prey into predator and the mortality of predator, respectively. In order to show the crowding effect, when the number of prey is large, the prey growth rate $f(x)$ in model (1.1) is usually a negative value. The most famous example of $xf(x)$ is the logistic form:

$$xf(x) = rx\left(1 - \frac{x}{K}\right), \tag{1.2}$$

where the positive constants r and K represent the inherent

growth rate of the prey and the carrying capacity of environment to the prey without the predator, respectively.

However, in the natural world, the factors influencing prey growth rate are not only limited to environmental carrying capacity K. The study of predator-prey interactions has become a significant research area because of its widespread occurrence. Numerous papers have been published, employing mathematical modeling to understand the complex dynamics of predator-prey systems. Predators have been observed to influence prey dynamics through direct predation [1, 2]. However, the impact of such predation on prey population is minimal [3, 4]. Although predators affect prey populations in various ways, the fear of predation leads to a significant decrease in the adaptive capacity of large populations [5, 6], even without predators killing individual members of the prey population. Moreover, fear alters prey behavior, which, in turn, can reduce reproductive output. Additionally, the presence of predator may change the behavioral patterns and physiological functions of prey, sometimes with more severe consequences than direct predation. In this paper, we assume that $xf(x)$ follows a logistic form influenced by the fear parameter$f$, as given by (1.3).

$$xf(x) = \frac{r_0 x}{1+fy} - dx - \frac{r_1 x^2}{K}, \tag{1.3}$$

where r_0 denotes the reproductive efficiency of the prey, f is the fear level caused by the predator to the prey, d is the natural mortality rate of the prey, and r_1 denotes the natural growth rate of the prey. Consequently, model (1.1) reads as

$$\begin{cases} \dfrac{dx}{dt} = \dfrac{r_0 x}{1+fy} - dx - \dfrac{r_1 x^2}{K} - g(x,y)y, \\ \dfrac{dy}{dt} = \epsilon g(x,y)y - \mu y. \end{cases} \tag{1.4}$$

The behavioral characteristics of the predator species can be reflected by the key element $g(x, y)$, referred to as the functional response or nutritional function. Ultimately, the functional response plays an important role in determining various dynamical behaviors, such as steady state, oscillation, bifurcation, and chaos [7]. In this paper, we choose the functional response function $g(x, y) = mx$, where m denotes the predator's capture rate. So our model is as follows

$$\begin{cases} \dfrac{dx}{dt} = \dfrac{r_0 x}{1+fy} - dx - \dfrac{r_1 x^2}{K} - mxy, \\ \dfrac{dy}{dt} = \epsilon mxy - \mu y. \end{cases} \tag{1.5}$$

A common phenomenon in predator-prey models is known as cooperative hunting among predators. This phenomenon causes the encountering rate between predators and prey to change with the number of predators [8–10]. Moreover, the efficiency of hunting may exhibit nonlinear dynamics as predator numbers increase [11–13]. However, when encountering a large aggregation of prey, extreme phenomena may occur, potentially leading to the extinction of the predator species. Therefore, Shang, Qiao, Duan, and Miao [14] added the constant yield harvest H to the first equation of model (1.5) to study the arrangement of renewable resources that ensures the coexistence of the two species.

$$\begin{cases} \dfrac{dx}{dt} = \dfrac{r_0 x}{1+fy} - dx - \dfrac{r_1 x^2}{K} - mxy - H, \\ \dfrac{dy}{dt} = \epsilon mxy - \mu y, \end{cases} \tag{1.6}$$

where the meanings of all parameters are presented in Table 1.

Table 1. Biological meanings of parameters in system (1.6).

Parameter	Meaning
x	Prey population density
y	Predator population density
$r_0 > 0$	Birth rate of prey population
$f > 0$	The level of fear by predator
$d > 0$	Death rate of prey population
$r_1 > 0$	Natality of prey population
$K > 0$	Carrying capacity of the environment to prey
$m > 0$	Predator's capture rate
$H > 0$	The constant yield harvest
$\epsilon > 0$	Conversion rate of prey into predator
$\mu > 0$	Death rate of predator

Since the death rate of the prey population in model (1.6) is given by $d = r_0 - r_1$, we will replace d with $r_0 - r_1$ in the subsequent models. By using the transformations $x = K\tilde{x}$, $y = \frac{\tilde{y}}{f}$, $t = \frac{\tilde{t}}{r_0}$, $a = \frac{r_1}{r_0}$, $b = \frac{m}{fr_0}$, $c = \frac{K\epsilon m}{r_0}$, $h = \frac{H}{r_0 K}$, $g = \frac{\mu}{r_0}$,

and dropping the bars in the above alphabets, we get the following predator-prey system:

$$\begin{cases} \dfrac{dx}{dt} = \dfrac{x}{1+y} - x + ax - ax^2 - bxy - h, \\ \dfrac{dy}{dt} = cxy - gy. \end{cases} \tag{1.7}$$

But considering the memorial nature of biological species, it is more suitable to adopt a fractional derivative to model the prey-predator system.

The concept of the fractional derivative dates back to the 18th century, with Liouville being the first mathematician to propose it [15]. In the 20th century, Riesz made further advancements by referencing the concept and exploring its properties [16]. His work, combined with that of Liouville, led to the establishment of the Riesz-Liouville definition of the fractional derivative, which remains in use today. Subsequently, Caputo introduced an alternative definition, now known as the Caputo fractional derivative [17], as follows:

Definition 1.1. *Denote*

$${}_0^C D_t^\alpha f(t) = J^{l-\alpha} f^{(l)}(t), \quad \alpha > 0,$$

where $f^{(l)}$ denotes the derivative of f with order l, l is the nearest integer to α, and J^q is the operator of the Riemann–Liouville integral of q order:

$$J^q h(t) = \frac{1}{\Gamma(q)} \int_0^t (t-\tau)^{q-1} h(\tau) d\tau,$$

where $\Gamma(q)$ is Euler's Gamma function. The alpha-order Caputo differential operator is the term used to describe the operator ${}_0^C D_t^\alpha$.

Fractional-order differential equations have attracted significant attention due to their capability to precisely describe various nonlinear phenomena. The development of models based on fractional-order differential equations has become increasingly popular in the study of dynamical systems [18, 19]. These models provide powerful mathematical tools for describing systems with memory effects and hereditary properties [20, 21]. Recently, an increasing number of researchers have focused on fractional-order biological models [22, 23], primarily because these equations inherently correspond to systems with memory—an essential characteristic of most biological systems—and are closely associated with fractals, which are prevalent in biological contexts [24, 25]. However, due to the limited theoretical tools available for analyzing the dynamics of fractional-order systems, the stability theory of fractional-order predator-prey models is still in its early stage.

In 2007, Ahmed [26] considered the following fractional-order predator-prey system:

$$\begin{cases} {}_0^C D_t^q x(t) = x(r - ax - by), \\ {}_0^C D_t^q y(t) = y(-d + cx), \end{cases} \tag{1.8}$$

where $0 < q \leq 1$, ${}_0^C D_t^q$ is the fractional derivative in the sense of Caputo, x and y represent prey and predator densities, respectively, and all constants r, a, b, c, and d are positive.

From a biological perspective, incorporating a fractional-order predator-prey system is justified. In fractional calculus, the rate of change at any given moment—represented by the fractional-order derivative—depends on population density over a certain time interval. This makes the fractional-order predator-prey model particularly effective for describing memory effect in a population.

Over the past two decades, the advantages of fractional derivative in capturing memory effects within ecological systems have attracted considerable attention from researchers, leading to extensive studies on fractional-order ecological models and the discovery of various dynamical properties [27–29]. Furthermore, fractional-order models offer distinct advantages in describing ecological processes with hereditary properties, yet their accuracy critically depends on the consistency with observational data. Although a relatively comprehensive framework has been established for integer-order ecosystems, the research on fractional-order ecosystems is still in an early stage. In this paper, we introduce the Caputo fractional derivative into system (1.7) and extend it into a fractional-order ecological model. Consequently, we obtain the following fractional-order predator-prey model

$$\begin{cases} {}_0^C D_t^\alpha x(t) = \dfrac{x}{1+y} - x + ax - ax^2 - bxy - h, \\ {}_0^C D_t^\alpha y(t) = cxy - gy, \end{cases} \tag{1.9}$$

which incorporates both fear effect and fixed harvest.

Currently, comprehensive dynamical analysis methods for continuous fractional-order predator-prey systems are lacking. Generally speaking, obtaining an exact solution for a complex differential equation or system is impossible. For example, as noted in [30], the analysis of fractional-order systems has primarily focused on the global asymptotic stability of the predator-extinction fixed point. Consequently, many researchers derive approximate solutions of corresponding systems by using computational methods.

Noticing that computers work on discrete points, it is practical and logical to discretize the corresponding continuous model. In [31], the authors examined various discretized predator-prey models and observed that these discrete models, compared with their continuous counterparts, demonstrate a broader range of dynamical behaviors and offer advantages in numerical simulations. In [32], the authors used the piecewise constant approximation (PCA) method to discretize a continuous fractional-order predator-prey system, analyzed its dynamical properties, and discussed the types of its bifurcations observed in the system. Their work motivates us to study the discrete version of system (1.9). Simultaneously, the advantages of the Predictor-Corrector Algorithm (PCA) for fractional-order ordinary differential dynamical systems are particularly remarkable. First, PCA avoids direct handling of the complex fractional-order integral kernel by transforming it into discrete summation. Second, for fractional-order systems, the PCA method exhibits superior numerical stability. Third, it supports variable step sizes and can be easily extended to higher-order approximations. Therefore, in this paper, we employ the PCA method to discretize model (1.9), with the steps outlined as follows.

Assume that the initial conditions of system (1.9) are $x(0) = x_0$ and $y(0) = y_0$. For a given step length ρ, denote $x(n\rho) = x_n$ and $y(n\rho) = y_n$ for $n = 0, 1, 2, \ldots$. The PCA method applied to system (1.9) is as follows:

$$\begin{cases} {}_0^C D_t^\alpha x(t) = \dfrac{x(\rho[t/\rho])}{1 + y(\rho[t/\rho])} - x(\rho[t/\rho]) + ax(\rho[t/\rho]) \\ \qquad\qquad - a(x(\rho[t/\rho]))^2 - bx(\rho[t/\rho])y(\rho[t/\rho]) - h, \\ {}_0^C D_t^\alpha y(t) = cx(\rho[t/\rho])y(\rho[t/\rho]) - gy(\rho[t/\rho]). \end{cases}$$

First, let $t \in [0, \rho)$, then $\frac{t}{\rho} \in [0, 1)$. Thus

$$\begin{cases} {}_0^C D_t^\alpha x_0(t) = \dfrac{x_0}{1 + y_0} - x_0 + ax_0 - ax_0^2 - bx_0y_0 - h, \\ {}_0^C D_t^\alpha y_0(t) = cx_0y_0 - gy_0. \end{cases} \tag{1.20}$$

Therefore, we obtain

$$\begin{aligned} x(t) &= x_0 + \mathcal{J}_{0\rho}^\alpha \left(\frac{x_0}{1 + y_0} - x_0 + ax_0 - ax_0^2 - bx_0y_0 - h \right) \\ &= x_0 + \frac{t^\alpha}{\alpha\Gamma(\alpha)} \left(\frac{x_0}{1 + y_0} - x_0 + ax_0 - ax_0^2 - bx_0y_0 - h \right), \\ y(t) &= y_0 + \mathcal{J}_{0\rho}^\alpha (cx_0y_0 - gy_0) \\ &= y_0 + \frac{t^\alpha}{\alpha\Gamma(\alpha)} (cx_0y_0 - gy_0). \end{aligned}$$

Second, let $t \in [\rho, 2\rho)$, then $\frac{t}{\rho} \in [1, 2)$. So,

$$\begin{cases} {}_0^C D_t^\alpha x_1(t) = \dfrac{x_1}{1 + y_1} - x_1 + ax_1 - ax_1^2 - bx_1y_1 - h, \\ {}_0^C D_t^\alpha y_1(t) = cx_1y_1 - gy_1. \end{cases} \tag{1.21}$$

After simplifying (1.21), we can obtain the following solution:

$$\begin{aligned} x(t) &= x_1 + \mathcal{J}_\rho^\alpha \left(\frac{x_1}{1 + y_1} - x_1 + ax_1 - ax_1^2 - bx_1y_1 - h \right) \\ &= x_1 + \frac{(t-\rho)^\alpha}{\alpha\Gamma(\alpha)} \left(\frac{x_1}{1 + y_1} - x_1 + ax_1 - ax_1^2 - bx_1y_1 - h \right), \\ y(t) &= y_1 + \mathcal{J}_\rho^\alpha (cx_1y_1 - gy_1) \\ &= y_1 + \frac{(t-\rho)^\alpha}{\alpha\Gamma(\alpha)} (cx_1y_1 - gy_1), \end{aligned}$$

where $\mathcal{J}_{k\rho}^\alpha = \frac{1}{\Gamma(\alpha)} \int_{k\rho}^t (t - \tau)^{\alpha-1} d\tau = \frac{(t-k\rho)^\alpha}{\alpha\Gamma(\alpha)}$, for $0 < \alpha < 1$, $t \in [k\rho, (k + 1)\rho]$, $k = 0, 1, 2, \ldots$. After n repetitions, we obtain

$$\begin{aligned} x(t) &= x_n + \frac{(t - n\rho)^\alpha}{\alpha\Gamma(\alpha)} \left(\frac{x_n}{1 + y_n} - x_n + ax_n - ax_n^2 - bx_ny_n - h \right), \\ y(t) &= y_n + \frac{(t - n\rho)^\alpha}{\alpha\Gamma(\alpha)} (cx_ny_n - gy_n), \end{aligned}$$

where $t \in [n\rho, (n + 1)\rho)$. Letting $t \to ((n + 1)\rho)^-$, the above system reads

$$\begin{cases} x_{n+1} = x_n + \dfrac{\rho^\alpha}{\Gamma(\alpha + 1)} \left(\dfrac{x_n}{1 + y_n} - x_n + ax_n - ax_n^2 - bx_ny_n - h \right), \\ y_{n+1} = y_n + \dfrac{\rho^\alpha}{\Gamma(\alpha + 1)} (cx_ny_n - gy_n). \end{cases} \tag{1.22}$$

System (1.22) is the model under discussion in this paper, where the parameters are the new dimensionless parameters derived from those mentioned in Table 1. The dynamical behavior of system (1.6) is similar to that of system (1.7) in phase space, due to their topological equivalence. Therefore, the study of the dimensionless system (1.7) will yield some properties that are equivalent to those of system (1.6).

The structure of this paper is outlined as follows: In Section 2, we provide some preliminaries, including some definitions, lemmas, and theorems that will be used to analyze the dynamical properties of system (1.22). In Section 3, we investigate the existence and stability of the fixed points of system (1.22). In Section 4, we demonstrate that, under certain parameter conditions, system (1.22) exhibits both a Neimark–Sacker bifurcation and a period-doubling bifurcation. In Section 5, we perform numerical simulations to validate the results of our theoretical analysis. Finally, in Section 6, we draw some interesting conclusions based on the findings presented in the previous sections.

2. Preliminaries

Definition 2.1. *([32]) Under the definition of Caputo fractional derivative, the fractional derivative of function $f(\xi) \in AC^n([0,+\infty],\mathbb{R})$ is given as*

$$ {}_0^C D_\xi^\alpha f(\xi) = \int_0^\xi \frac{f^{(n)}(\vartheta)}{\Gamma(n-\alpha)(\xi-\vartheta)^{\alpha-n+1}} d\vartheta, $$

where α represents the order of the fractional derivative and n is the nearest integer to α satisfying $n < \alpha \le n+1$.

When $n = 1$, the fractional derivative ${}_0^C D_\xi^\alpha f(\xi)$ takes the form of

$$ {}_0^C D_\xi^\alpha f(\xi) = \int_0^\xi \frac{f'(\vartheta)}{\Gamma(1-\alpha)(\xi-\vartheta)^{\alpha}} d\vartheta. $$

Definition 2.2. *([32]) The Mittag-Leffler function M_i, when the order i of M_i is positive, is defined as*

$$ M_i(\zeta) = \sum_{j=0}^{\infty} \frac{\zeta_j}{\Gamma(ji+1)}, \quad \zeta_j \in \mathbb{C} $$

when the series converges.

Definition 2.3. *([33]) Let $Q(x,y)$ be a fixed point of system (1.6) with multipliers λ_1 and λ_2.*

(i) If $|\lambda_1| < 1$ and $|\lambda_2| < 1$, then the fixed point $Q(x,y)$ is called a sink, and a sink is locally asymptotically stable.

(ii) If $|\lambda_1| > 1$ and $|\lambda_2| > 1$, then the fixed point $Q(x,y)$ is called a source, and a source is locally unstable.

(iii) If $|\lambda_1| < 1$ and $|\lambda_2| > 1$ (or $|\lambda_1| > 1$ and $|\lambda_2| < 1$), then the fixed point $Q(x,y)$ is called a saddle.

(iv) If either $|\lambda_1| = 1$ or $|\lambda_2| = 1$, then the fixed point $Q(x,y)$ is called non-hyperbolic.

Lemma 2.1. *Let $F(\lambda) = \lambda^2 + B\lambda + C$, where B and C are two real constants. Suppose λ_1 and λ_2 are two roots of $F(\lambda) = 0$. Then the following statements hold.*

(i) If $F(1) > 0$, then

(i.1) $|\lambda_1| < 1$ and $|\lambda_2| < 1$ if and only if $F(-1) > 0$ and $C < 1$;

(i.2) $\lambda_1 = -1$ and $\lambda_2 \neq -1$ if and only if $F(-1) = 0$ and $B \neq 2$;

(i.3) $|\lambda_1| < 1$ and $|\lambda_2| > 1$ if and only if $F(-1) < 0$;

(i.4) $|\lambda_1| > 1$ and $|\lambda_2| > 1$ if and only if $F(-1) > 0$ and $C > 1$;

(i.5) λ_1 and λ_2 are a pair of conjugate complex roots and $|\lambda_1| = |\lambda_2| = 1$ if and only if $-2 < B < 2$ and $C = 1$;

(i.6) $\lambda_1 = \lambda_2 = -1$ if and only if $F(-1) = 0$ and $B = 2$.

(ii) If $F(1) = 0$, namely, 1 is one root of $F(\lambda) = 0$, then the other root λ satisfies $|\lambda| = (>,<)1$ if and only if $|C| = (>,<)1$.

(iii) If $F(1) < 0$, then $F(\lambda) = 0$ has one root lying in $(1,\infty)$. Moreover,

(iii.1) The other root λ satisfies $\lambda = (>,<)-1$ if and only if $F(-1) = (>,<)0$;

(iii.2) The other root $-1 < \lambda < 1$ if and only if $F(-1) > 0$.

3. Existence and stability of fixed points

3.1. Existence of fixed points

In this section, we first consider the existence of fixed points of system (1.22) and then analyze the local stability of these fixed points.

The fixed points of system (1.22) satisfy the following equations

$$\begin{cases} x = x + \dfrac{\rho^\alpha}{\Gamma(\alpha+1)}\left(\dfrac{x}{1+y} - x + ax - ax^2 - bxy - h\right), \\ y = y + \dfrac{\rho^\alpha}{\Gamma(\alpha+1)}\left(cxy - gy\right), \end{cases} \tag{3.1}$$

namely,

$$\begin{cases} \dfrac{x}{1+y} - x + ax - ax^2 - bxy - h = 0, \\ cxy - gy = 0. \end{cases} \tag{3.2}$$

Considering the biological meanings of system (1.22), we only take into account its nonnegative fixed points. Proceeding step by step, we begin with the relatively simple boundary fixed points. Because $h > 0$, it follows from the first equation of (3.2) that system (1.22) has no boundary fixed points of type $(0, y)$. Now consider boundary fixed points of type $(x, 0)$.

When $y = 0$, in the view of the first equation in (3.2), one has $ax - ax^2 - h = 0$. Therefrom, we have,

(i) if $h > \frac{a}{4}$, then $ax - ax^2 - h < 0$ for any $x \geq 0$, hence system (1.22) has no boundary fixed points of type $(x, 0)$;

(ii) if $h = \frac{a}{4}$, then $ax - ax^2 - h = 0$ if and only if $x = \frac{1}{2}$, so system (1.22) has a unique predator-free fixed point $E_0\left(\frac{1}{2}, 0\right)$;

(iii) if $0 < h < \frac{a}{4}$, then $ax - ax^2 - h = 0$ has two positive roots $x = \frac{1 \pm \sqrt{1-\frac{4h}{a}}}{2}$, hence system (1.22) has two boundary fixed points $E_1\left(\frac{1-\sqrt{1-\frac{4h}{a}}}{2}, 0\right)$ and $E_2\left(\frac{1+\sqrt{1-\frac{4h}{a}}}{2}, 0\right)$.

Therefore, for boundary fixed points of system (1.22), one has the following result.

Theorem 3.1. *System (1.22) has no boundary fixed points of type $(0, y)$. As for boundary fixed point of type $(x, 0)$, for $h > \frac{a}{4}$, system (1.22) has no boundary fixed points of type $(x, 0)$; for $h = \frac{a}{4}$, system (1.22) has a unique predator-free fixed point $E_0\left(\frac{1}{2}, 0\right)$; for $0 < h < \frac{a}{4}$, system (1.22) has two boundary fixed point $E_1\left(\frac{1-\sqrt{1-\frac{4h}{a}}}{2}, 0\right)$ and $E_2\left(\frac{1+\sqrt{1-\frac{4h}{a}}}{2}, 0\right)$.*

Next, we analyze the existence of positive fixed points of system (1.22). When $y > 0$, it follows from the second equation of (3.2) that $x = \frac{g}{c}$. Substituting this expression into the first equation of (3.2), we obtain the following quadratic equation

$$y^2 + (P + \frac{b+1}{b})y + P = 0, \tag{3.3}$$

where $P = \frac{-acg + ag^2 + c^2 h}{bcg}$. Obviously, the discriminant quantity of (3.3) $\Delta = (P + \frac{b+1}{b})^2 - 4P = (P + \frac{1-b}{b})^2 + \frac{4}{b} > 0$. So the Eq (3.3) always has two real roots. We are only interested in its positive roots.

Notice $P = \frac{-acg + ag^2 + c^2 h}{bcg} > (=, <) 0 \Leftrightarrow h > (=, <) \frac{ag(c-g)}{c^2}$. Then,

(i) for $c \leq g$ or $c > g$ and $h \geq \frac{ag(c-g)}{c^2}$, $P > 0$. So, system (1.22) has no positive fixed points.

(ii) for $c > g$ and $0 < h < \frac{ag(c-g)}{c^2}$, $P < 0$. Then system (1.22) has a unique positive fixed point E_3 $(\frac{g}{c}, \frac{1}{2}[\sqrt{(P + \frac{b+1}{b})^2 - 4P} - (\frac{b+1}{b} + P)])$.

Summarizing the above analysis, we have

Theorem 3.2. *When $c \leq g$ or $c > g$ and $h \geq \frac{ag(c-g)}{c^2}$, system (1.22) has no positive fixed points; for $c > g$ and $0 < h < \frac{ag(c-g)}{c^2}$, system (1.22) has a unique positive fixed point E_3 $(\frac{g}{c}, \frac{1}{2}[\sqrt{(P + \frac{b+1}{b})^2 - 4P} - (\frac{b+1}{b} + P)])$, where $P = \frac{-acg + ag^2 + c^2 h}{bcg}$. The existence conditions for all nonnegative fixed points of system (1.22) are summarized in Table 2.*

Table 2. The existence of fixed point.

Conditions	Type of fixed point	Coordinate of fixed point
$h > \frac{a}{4}$	nonexistence of type $(x, 0)$	
$h = \frac{a}{4}$	a unique predator-free fixed point	$E_0\left(\frac{1}{2}, 0\right)$
$0 < h < \frac{a}{4}$	two boundary fixed point	$E_1\left(\frac{1-\sqrt{1-\frac{4h}{a}}}{2}, 0\right)$, $E_2\left(\frac{1+\sqrt{1-\frac{4h}{a}}}{2}, 0\right)$
$c \leq g$ or $c > g$ and $h \geq \frac{ag(c-g)}{c^2}$	no positive fixed point	
$c > g$ and $0 < h < \frac{ag(c-g)}{c^2}$	a unique positive fixed point	$E_3\left(\frac{g}{c}, \frac{1}{2}[\sqrt{(P + \frac{b+1}{b})^2 - 4P} - (\frac{b+1}{b} + P)]\right)$

3.2. Stability of fixed points

Now, we begin to analyze the stability of these fixed points. The Jacobian matrix J of system (1.22) at a fixed point $E(x, y)$ is presented as follows:

$$J(E) = \begin{pmatrix} 1 + \delta\psi_1(y) & -\delta x\psi_2(y) \\ \delta cy & 1 + \delta(cx - g) \end{pmatrix}, \tag{3.4}$$

where $\delta = \dfrac{\rho^\alpha}{\Gamma(\alpha+1)}$, $\psi_1(y) = \dfrac{1}{1+y} - 1 + a - 2ax - by$, $\psi_2(y) = \dfrac{1}{(1+y)^2} + b$.

The characteristic equation of the Jacobian matrix $J(E)$ can be written as

$$\lambda^2 - p(x,y)\lambda + q(x,y) = 0, \tag{3.5}$$

here, $p(x,y) = \mathrm{tr}(E)$ while $q(x,y)$ is the determinant of $J(E)$:

$$p(x,y) = 2 + \frac{\rho^\alpha}{\Gamma(\alpha+1)}\left(\frac{1}{1+y} - 1 + a - 2ax - by + cx - g\right),$$

$$\begin{aligned} q(x,y) = 1 &+ \frac{\rho^\alpha}{\Gamma(\alpha+1)}\left(\frac{1}{1+y} - 1 + a - 2ax - by + cx - g\right) \\ &+ \frac{\rho^{2\alpha}}{\Gamma^2(\alpha+1)}\left(\frac{1}{1+y} - 1 + a - 2ax - by\right)(cx - g) \\ &+ \frac{\rho^{2\alpha} cy}{\Gamma^2(\alpha+1)}\left(\frac{x}{(1+y)^2} + bx\right). \end{aligned}$$

Now, denote $\delta = \frac{\rho^\alpha}{\Gamma(\alpha+1)}$. For the stability of fixed points $E_0\left(\frac{1}{2}, 0\right)$, $E_1\left(\frac{1-\sqrt{1-\frac{4h}{a}}}{2}, 0\right)$, $E_2\left(\frac{1+\sqrt{1-\frac{4h}{a}}}{2}, 0\right)$, and $E_3(\frac{g}{c}, \frac{1}{2}[\sqrt{(P+\frac{b+1}{b})^2 - 4P} - (\frac{b+1}{b} + P)])$, we can easily get the following Theorems 3.3–3.5, respectively.

Theorem 3.3. *The fixed point $E_0 = \left(\frac{1}{2}, 0\right)$ of system (1.22) is non-hyperbolic.*

Theorem 3.4. *For $0 < h < \frac{a}{4}$, the boundary fixed point $E_1(x_1, 0) = E_1\left(\frac{1-\sqrt{1-\frac{4h}{a}}}{2}, 0\right)$ of system (1.22) occurs. The results in the following Table 3 about the fixed point E_1 are true.*

Table 3. Properties of the fixed point E_1.

Conditions		Eigenvalues	Properties
$\frac{g}{c} < \frac{1-\sqrt{1-\frac{4h}{a}}}{2}$		$\lvert\lambda_1\rvert > 1, \lvert\lambda_2\rvert > 1$	unstable node
$\frac{g}{c} = \frac{1-\sqrt{1-\frac{4h}{a}}}{2}$		$\lvert\lambda_1\rvert = 1$ or $\lvert\lambda_2\rvert = 1$	non-hyperbolic
	$0 < \delta < \frac{2}{g-cx_1}$	$\lvert\lambda_1\rvert > 1, \lvert\lambda_2\rvert < 1$	saddle
$\frac{g}{c} > \frac{1-\sqrt{1-\frac{4h}{a}}}{2}$	$\delta = \frac{2}{g-cx_1}$	$\lvert\lambda_1\rvert = 1$ or $\lvert\lambda_2\rvert = 1$	non-hyperbolic
	$\delta > \frac{2}{g-cx_1}$	$\lvert\lambda_1\rvert > 1, \lvert\lambda_2\rvert > 1$	source

Theorem 3.5. *For $0 < h < \frac{a}{4}$, system (1.22) has the boundary fixed point $E_2(x_2, 0) = E_2\left(\frac{1+\sqrt{1-4\frac{h}{a}}}{2}, 0\right)$. The following results are valid for the fixed point E_2.*

(i) For $\frac{g}{c} < \frac{1+\sqrt{1-\frac{4h}{a}}}{2}$, the related conclusions are presented in Table 4.

Table 4. Properties of the fixed point E_2 when $\frac{g}{c} < \frac{1+\sqrt{1-\frac{4h}{a}}}{2}$.

Conditions		Eigenvalues	Properties
	$0 < \delta < \frac{2}{\sqrt{a^2-4ah}}$	$\lvert\lambda_1\rvert > 1, \lvert\lambda_2\rvert < 1$	saddle
$\frac{g}{c} < \frac{1+\sqrt{1-\frac{4h}{a}}}{2}$	$\delta = \frac{2}{\sqrt{a^2-4ah}}$	$\lvert\lambda_1\rvert = 1$ or $\lvert\lambda_2\rvert = 1$	non-hyperbolic
	$\frac{2}{\sqrt{a^2-4ah}} < \delta$	$\lvert\lambda_1\rvert > 1, \lvert\lambda_2\rvert > 1$	unstable node

(ii) for $\frac{g}{c} = \frac{1+\sqrt{1-\frac{4h}{a}}}{2}$, the boundary fixed point E_2 is non-hyperbolic.

(iii) for $\frac{g}{c} > \frac{1+\sqrt{1-\frac{4h}{a}}}{2}$, the related conclusions are presented in Table 5.

Table 5. Properties of the fixed point E_2 when $\frac{g}{c} > \frac{1+\sqrt{1-\frac{4h}{a}}}{2}$.

Conditions		Eigenvalues	Properties
	$0 < \delta < \frac{2}{\sqrt{a^2-4ah}}$	$\lvert\lambda_1\rvert < 1, \lvert\lambda_2\rvert < 1$	stable node
	$\delta = \frac{2}{\sqrt{a^2-4ah}}$	$\lvert\lambda_1\rvert = 1$ or $\lvert\lambda_2\rvert = 1$	non-hyperbolic
$g - cx_2 < \sqrt{a^2-4ah}$	$\frac{2}{\sqrt{a^2-4ah}} < \delta < \frac{2}{g-cx_2}$	$\lvert\lambda_1\rvert > 1, \lvert\lambda_2\rvert < 1$	saddle
	$\delta = \frac{2}{g-cx_2}$	$\lvert\lambda_1\rvert = 1$ or $\lvert\lambda_2\rvert = 1$	non-hyperbolic
	$\frac{2}{g-cx_2} < \delta$	$\lvert\lambda_1\rvert > 1, \lvert\lambda_2\rvert > 1$	unstable node
	$0 < \delta < \frac{2}{g-cx_2}$	$\lvert\lambda_1\rvert < 1, \lvert\lambda_2\rvert < 1$	stable node
$g - cx_2 = \sqrt{a^2-4ah}$	$\delta = \frac{2}{\sqrt{a^2-4ah}}$	$\lvert\lambda_1\rvert = 1$ or $\lvert\lambda_2\rvert = 1$	non-hyperbolic
	$\frac{2}{\sqrt{a^2-4ah}} < \delta$	$\lvert\lambda_1\rvert > 1, \lvert\lambda_2\rvert > 1$	unstable node
	$0 < \delta < \frac{2}{g-cx_2}$	$\lvert\lambda_1\rvert < 1, \lvert\lambda_2\rvert < 1$	stable node
	$\delta = \frac{2}{\sqrt{a^2-4ah}}$	$\lvert\lambda_1\rvert = 1$ or $\lvert\lambda_2\rvert = 1$	non-hyperbolic
$g - cx_2 > \sqrt{a^2-4ah}$	$\frac{2}{g-cx_2} < \delta < \frac{2}{\sqrt{a^2-4ah}}$	$\lvert\lambda_1\rvert > 1, \lvert\lambda_2\rvert < 1$	saddle
	$\delta = \frac{2}{\sqrt{a^2-4ah}}$	$\lvert\lambda_1\rvert = 1$ or $\lvert\lambda_2\rvert = 1$	non-hyperbolic
	$\frac{2}{\sqrt{a^2-4ah}} < \delta$	$\lvert\lambda_1\rvert > 1, \lvert\lambda_2\rvert > 1$	unstable node

Theorem 3.6. *For $c > g$ and $0 < h < \frac{ag(c-g)}{c^2}$, the unique positive fixed point E_3 of system (1.22) occurs. Put $E_3(x_3, y_3) = E_3(\frac{g}{c}, \frac{1}{2}[\sqrt{(P+\frac{b+1}{b})^2 - 4P} - (\frac{b+1}{b} + P)])$, $A = \frac{hc}{g} - \frac{ag}{c}$ and $B = \frac{gy_3}{(1+y_3)^2} + bgy_3$. Then the results stated in the Table 6 are true.*

Table 6. Properties of the fixed point E_3 of system (1.22).

Conditions			Eigenvalues	Properties
$h \le \frac{ag^2}{c^2}$			$\lvert\lambda_1\rvert > 1, \lvert\lambda_2\rvert > 1$	unstable node
$h > \frac{ag^2}{c^2}$	$4B > A^2$	$0 < \delta < \frac{A}{B}$	$\lvert\lambda_1\rvert < 1, \lvert\lambda_2\rvert < 1$	stable node
		$\delta = \frac{A}{B}$	$\lvert\lambda_1\rvert = 1$ or $\lvert\lambda_2\rvert = 1$	non-hyperbolic
		$\frac{A}{B} < \delta$	$\lvert\lambda_1\rvert > 1, \lvert\lambda_2\rvert > 1$	unstable node
	$4B = A^2$	$0 < \delta < \frac{A}{B}$	$\lvert\lambda_1\rvert < 1, \lvert\lambda_2\rvert < 1$	stable node
		$\delta = \frac{A}{B}$	$\lvert\lambda_1\rvert = 1$ or $\lvert\lambda_2\rvert = 1$	non-hyperbolic
		$\frac{A}{B} < \delta$	$\lvert\lambda_1\rvert > 1, \lvert\lambda_2\rvert > 1$	unstable node
	$4B < A^2$	$0 < \delta < \frac{A-\sqrt{A^2-B^2/4}}{B}$	$\lvert\lambda_1\rvert < 1, \lvert\lambda_2\rvert < 1$	stable node
		$\delta = \frac{A-\sqrt{A^2-B^2/4}}{B}$	$\lvert\lambda_1\rvert = 1$ or $\lvert\lambda_2\rvert = 1$	non-hyperbolic
		$\frac{A-\sqrt{A^2-B^2/4}}{B} < \delta < \frac{A+\sqrt{A^2-B^2/4}}{B}$	$\lvert\lambda_1\rvert < (>)1, \lvert\lambda_2\rvert > (<)1$	saddle
		$\delta = \frac{A+\sqrt{A^2-B^2/4}}{B}$	$\lvert\lambda_1\rvert = 1$ or $\lvert\lambda_2\rvert = 1$	non-hyperbolic
		$\frac{A+\sqrt{A^2-B^2/4}}{B} < \delta$	$\lvert\lambda_1\rvert > 1, \lvert\lambda_2\rvert > 1$	unstable node

Proof. Notice that $c > g$ and $0 < h < \frac{ag(c-g)}{c^2}$ imply $B > 0$. The condition $A > (=, <)0$ depends on $h > (=, <)\frac{ag^2}{c^2}$.

The Jacobian matrix of system (1.22) at the fixed point E_3 may be simplified into

$$J(E_3) = \begin{pmatrix} 1 - A\delta & -\delta(\frac{g}{c(1+y_3)^2} - \frac{bg}{c}) \\ \delta c y_3 & 1 \end{pmatrix},$$

hence we obtain the characteristic polynomial of the Jacobian matrix $J(E_3)$

$$F(\lambda) = \lambda^2 - p\lambda + q,$$

where

$$p = 2 - A\delta, \quad q = 1 - A\delta + B\delta^2.$$

It is clear that

$$F(1) = B\delta^2 > 0 \quad \text{and} \quad F(-1) = B\delta^2 - 2A\delta + 4.$$

When $h \le \frac{ag^2}{c^2}$, $A \le 0$. At this time, $q > 1$, $F(-1) > 0$ and $\delta > \frac{A}{B}$ are obvious. Therefore, according to Lemma 2.1, we know that E_3 is an unstable node, i.e., a source.

When $h > \frac{ag^2}{c^2}$, $A > 0$ and $c > 2g$. Notice that $q > (=, <)1 \iff \delta > (=, <)\frac{A}{B}$. Now, consider the following three cases.

Case 1: $B > \frac{A^2}{4}$. Then $F(-1) > 0$ always holds. Consider the following three subcases:

Subcase 1: $\delta < \frac{A}{B}$. Then, $q < 1$. Lemma 2.1 reads $|\lambda_1| < 1$ and $|\lambda_2| < 1$. Thus, E_3 is a stable node, i.e., a sink.

Subcase 2: $\delta = \frac{A}{B}$. Then, $q = 1$, $-2 < p < 2$, Thus, $|\lambda_1| = 1$ or $|\lambda_2| = 1$, so E_3 is non-hyperbolic.

Subcase 3: $\delta > \frac{A}{B}$. Then, $q > 1$. Thus, $|\lambda_1| > 1$, $|\lambda_2| > 1$, indicating E_3 is an unstable node, i.e., a source.

Case 2: $B = \frac{A^2}{4}$. Consider the following three subcases:

Subcase 1: $\delta < \frac{A}{B}$. Then, $F(-1) > 0$, $q < 1$. Hence, $|\lambda_1| < 1$, $|\lambda_2| < 1$, which shows that E_3 is a stable node, i.e., a sink.

Subcase 2: $\delta = \frac{A}{B}$. Then, $F(-1) = 0$, Thus, $|\lambda_1| = 1$ or $|\lambda_2| = 1$, implying E_3 is non-hyperbolic.

Subcase 3: $\delta > \frac{A}{B}$. Then, $F(-1) > 0$ and $q > 1$. It follows from Lemma 2.1 (i.4) that $|\lambda_1| > 1$ and $|\lambda_2| > 1$. Thus, E_3 is an unstable node, i.e., a source.

Case 3: $B < \frac{A^2}{4}$. Consider the following five subcases:

Subcase 1: $0 < \delta < \frac{A-\sqrt{A^2-4B}}{B}$. Then, $F(-1) > 0$, $q < 1$, indicating $|\lambda_1| < 1$, $|\lambda_2| < 1$. Hence, E_3 is a stable node, i.e., a sink.

Subcase 2: $\delta = \frac{A-\sqrt{A^2-4B}}{B}$. Then, $F(-1) = 0$, Thus, $|\lambda_1| = 1$ or $|\lambda_2| = 1$, means that reads E_3 is non-hyperbolic.

Subcase 3: $\frac{A-\sqrt{A^2-4B}}{B} < \delta < \frac{A+\sqrt{A^2-4B}}{B}$. Then, $F(-1) < 0$. Hence, E_3 is a saddle.

Subcase 4: $\delta = \frac{A+\sqrt{A^2-4B}}{B}$. Then, $F(-1) = 0$, Thus, $|\lambda_1| = 1$ or $|\lambda_2| = 1$, hence E_3 is non-hyperbolic.

Subcase 5: $\delta > \frac{A+\sqrt{A^2-4B}}{B}$. Then, $F(-1) > 0$, $q > 1$ and so $|\lambda_1| > 1$, $|\lambda_2| > 1$. Therefore, E_3 is an unstable node, i.e., a source. The proof is finished. □

4. Bifurcation analysis

In this section, we apply the center manifold theorem and local bifurcation theory to primarily study the local bifurcation problems of system (1.22) at the fixed point $E_3(x_3, y_3)$, considering its practical biological meaning.

4.1. Neimark–Sacker bifurcation at the fixed point E_3

From Case 1 in the proof of Theorem 3.6 for the stability of the positive fixed point $E_3(x_3, y_3)$, we see that the dimension numbers for the stable manifold and unstable manifold of system (1.22) at the positive fixed point E_3 change when δ varies in the vicinity of δ_0 (correspondingly, ρ varies in the vicinity of ρ_0) for $4B > A^2$, where

$$\delta_0 = \frac{A}{B}, \quad \rho_0 = (\Gamma(\alpha + 1)\delta_0)^{\frac{1}{\alpha}}. \tag{4.1}$$

Thus, a bifurcation, to be shown to be a Neimark–Sacker bifurcation later, may occur. Denote

$$S=\{(a,b,c,g,h,\alpha,\rho)\in\mathbb{R}^5_+|c>g,0<h<\frac{ag(c-g)}{c^2},B>\frac{A^2}{4}\}.$$

To analyze the Neimark–Sacker bifurcation, we perform the following process.

Let $X_n = x_n - x_3$ and $Y_n = y_n - y_3$, which transforms the fixed point E_3 to the origin $O(0,0)$. Assume that ρ^* is a small perturbation of ρ, i.e., $\rho^* = \rho - \rho_0$, with $0 < |\rho^*| \ll 1$. After shifting and perturbation, system (1.22) takes the following form

$$\begin{cases} X_{n+1} = X_n + \dfrac{(\rho_0+\rho_*)^\alpha}{\Gamma(\alpha+1)}\Big(\dfrac{X_n+x_3}{1+Y_n+y_3} - (X_n+x_3) \\ \qquad + a(X_n+x_3) - a(X_n+x_3)^2 - b(X_n+x_3)(Y_n+y_3) - h\Big), \\ Y_{n+1} = Y_n + \dfrac{(\rho_0+\rho_*)^\alpha}{\Gamma(\alpha+1)}\left(c(X_n+x_3)(Y_n+y_3) - g(Y_n+y_3)\right). \end{cases} \tag{4.2}$$

Taylor expanding of system (4.2) at $(X,Y)=(0,0)$

$$\begin{cases} X_{n+1} = a_{10}X_n + a_{01}Y_n + a_{20}X_n^2 + a_{11}X_nY_n + a_{02}Y_n^2 \\ \qquad + a_{30}X_n^3 + a_{21}X_n^2Y_n + a_{12}X_nY_n^2 + a_{03}Y_n^3 + o(\rho_1^3), \\ Y_{n+1} = b_{10}X_n + b_{01}Y_n + b_{20}X_n^2 + b_{11}X_nY_n + b_{02}Y_n^2 \\ \qquad + b_{30}X_n^3 + b_{21}X_n^2Y_n + b_{12}X_nY_n^2 + b_{03}Y_n^3 + o(\rho_1^3), \end{cases} \tag{4.3}$$

where $\rho_1 = \sqrt{X_n^2+Y_n^2}$,

$$a_{10} = -\left(\frac{\rho^\alpha}{\Gamma(\alpha+1)}\left(2ax_3 - \frac{1}{y_3+1} - a + by_3 + 1\right) - 1\right),$$
$$a_{01} = -\frac{\rho^\alpha}{\Gamma(\alpha+1)}\left(\frac{x_3}{(y_3+1)^2} + bx_3\right),$$
$$a_{20} = -\frac{\rho^\alpha a}{\Gamma(\alpha+1)}, a_{02} = \frac{\rho^\alpha}{\Gamma(\alpha+1)}\frac{x_3}{(y_3+1)^3},$$
$$a_{30} = 0, \quad a_{03} = -\frac{\rho^\alpha}{\Gamma(\alpha+1)}\frac{x_3}{(y_3+1)^4},$$
$$a_{11} = -\frac{\rho^\alpha}{\Gamma(\alpha+1)}\left(b + \frac{1}{(y_3+1)^2}\right), a_{21} = 0,$$
$$a_{12} = \frac{\rho^\alpha}{\Gamma(\alpha+1)}\frac{1}{(y_3+1)^2}, b_{10} = \frac{cy_3\rho^\alpha}{\Gamma(\alpha+1)}, \quad b_{11} = \frac{c\rho^\alpha}{\Gamma(\alpha+1)},$$
$$b_{01} = b_{20} = b_{02} = b_{30} = b_{03} = b_{21} = b_{12} = 0.$$

The characteristic equation of linearized equation associated with Eq (4.3) at $(0,0)$ is

$$F(\lambda) = \lambda^2 - p(\rho^*)\lambda + q(\rho^*),$$

among which

$$p = 2-A\delta(\rho^*),\ q = 1-A\delta(\rho^*)+B\delta(\rho^*)^2,\ \delta(\rho^*) = \frac{(\rho_0+\rho^*)^\alpha}{\Gamma(\alpha+1)}.$$

Evidently,

$$\lambda_{1,2}(\rho^*) = \frac{p(\rho^*) \pm i\sqrt{4q(\rho^*) - p^2(\rho^*)}}{2}.$$

Moreover,

$$(|\lambda_{1,2}(\rho^*)|)_{\rho^*=0} = \sqrt{q(\rho^*)}\Big|_{\rho^*=0} = 1,$$

$$\left(\frac{d|\lambda_{1,2}(\rho^*)|}{d\rho^*}\right)_{\rho^*=0} = \frac{\alpha\rho_0^{\alpha-1}A}{2\Gamma(\alpha+1)} \neq 0.$$

It is obvious that $\lambda_{1,2}^i(0) \neq 1$ for $i = 1,2,3,4$. Thus, the transversal and nondegenerate conditions hold for a Neimark–Sacker bifurcation to occur.

In order to derive the normal form of system (4.3), let

$$T = \begin{pmatrix} 0 & a_{01} \\ \mu & 1-\omega \end{pmatrix},$$

in which $\omega = -\frac{p(\rho^*)}{2}$, $\mu = \sqrt{\frac{4q(\rho^*)-p^2(\rho^*)}{2}}$. Then, we have

$$T^{-1} = \begin{pmatrix} \frac{\omega-1}{\mu a_{01}} & \frac{1}{\mu} \\ \frac{1}{a_{01}} & 0 \end{pmatrix}.$$

Take the following transformation:

$$(X,Y)^T = T(U,V)^T,$$

then, system (4.3) takes the following form

$$\begin{pmatrix} U \\ V \end{pmatrix} \to \begin{pmatrix} \omega-\mu & \mu \\ \mu & \omega \end{pmatrix}\begin{pmatrix} U \\ V \end{pmatrix} + \left(\begin{pmatrix} F(U,V) \\ G(U,V) \end{pmatrix} + o(\rho_2^3)\right), \tag{4.4}$$

where $\rho_2 = \sqrt{x_n^2+y_n^2}$,

$$\begin{aligned} F(U,V) = {} & c_{20}X^2 + c_{11}XY + c_{02}Y^2 + c_{30}X^3 \\ & + c_{21}X^2Y + c_{12}XY^2 + c_{03}Y^3, \end{aligned} \tag{4.1}$$

$$\begin{aligned} G(U,V) = {} & d_{20}X^2 + d_{11}XY + d_{02}Y^2 + d_{30}X^3 \\ & + d_{21}X^2Y + d_{12}XY^2 + d_{03}Y^3, \end{aligned} \tag{4.2}$$

with $X = a_{01}V$ and $Y = \mu U + (1-\omega)V$,

$$c_{20} = \frac{a_{20}(\omega-1)}{\mu a_{01}} + \frac{b_{20}}{\mu}, \quad c_{02} = \frac{a_{02}(\omega-1)}{\mu a_{01}} + \frac{b_{02}}{\mu},$$

$$c_{11} = \frac{a_{11}(\omega-1)}{\mu a_{01}} + \frac{a_{11}}{\mu}, c_{21} = \frac{a_{21}(\omega-1)}{\mu a_{01}} + \frac{b_{21}}{\mu},$$
$$c_{30} = \frac{a_{30}(\omega-1)}{\mu a_{01}} + \frac{b_{30}}{\mu}, c_{03} = \frac{a_{03}(\omega-1)}{\mu a_{01}} + \frac{b_{03}}{\mu},$$
$$c_{12} = \frac{a_{12}(\omega-1)}{\mu a_{01}} + \frac{b_{12}}{\mu}, d_{20} = \frac{a_{20}}{a_{01}}, d_{02} = \frac{a_{02}}{a_{01}}, d_{11} = \frac{a_{11}}{a_{01}},$$
$$d_{30} = \frac{a_{30}}{a_{01}}, \quad d_{03} = \frac{a_{03}}{a_{01}}, \quad d_{21} = \frac{a_{21}}{a_{01}}, \quad d_{12} = \frac{a_{12}}{a_{01}}.$$

Moreover,

$$\begin{aligned}
F_{UU}|_{(0,0)} &= 2c_{02}\mu^3, \ F_{UV}|_{(0,0)} = c_{11}a_{01}\mu + 2c_{02}\mu(1-\omega),\\
F_{VV}|_{(0,0)} &= 2c_{20}a_{01}^2 + 2c_{11}a_{01}(1-\omega), \ F_{UUU}|_{(0,0)} = 6c_{03}\mu^3,\\
F_{UUV}|_{(0,0)} &= 2c_{21}a_{01}\mu^2 + 6c_{03}\mu^2(1-\omega),\\
F_{UVV}|_{(0,0)} &= 2c_{21}a_{01}^2\mu + 4c_{12}a_{01}\mu(1-\omega) + 6c_{03}\mu(1-\omega)^2,\\
F_{VVV}|_{(0,0)} &= 4(1-\omega)^3 + 6c_{30}a_{01}^3\\
&\quad + 4c_{21}a_{01}^2(1-\omega) + 6c_{12}a_{01}(1-\omega)^2,\\
G_{UU}|_{(0,0)} &= 2d_{02}\mu^3, \quad G_{UV}|_{(0,0)} = d_{11}a_{01}\mu + 2d_{02}\mu(1-\omega),\\
G_{VV}|_{(0,0)} &= 2d_{20}a_{01} + 2d_{11}a_{01}(1-\omega), \ G_{UUU}|_{(0,0)} = 6d_{03}\mu^3,\\
G_{UUV}|_{(0,0)} &= 2d_{21}a_{01}\mu^2 + 6d_{03}\mu^2(1-\omega),\\
G_{UVV}|_{(0,0)} &= 2d_{21}a_{01}^2\mu + 4d_{12}a_{01}\mu(1-\omega) + 6d_{03}\mu(1-\omega)^2,\\
G_{VVV}|_{(0,0)} &= 4(1-\omega)^3 + 6d_{30}a_{01}^3\\
&\quad + 4d_{21}a_{01}^2(1-\omega) + 6d_{12}a_{01}(1-\omega)^2.
\end{aligned}$$

In order to ensure that system (1.22) undergoes a Neimark-Sacker bifurcation and to determine the stability and direction of the bifurcation curve, the discriminant L must be calculated and should not be equal to zero, where

$$\begin{aligned}
L = &-\mathrm{Re}\left(\frac{(1-2\lambda_1)\lambda_2^2\tau_{20}\tau_{11}}{1-\lambda_1}\right)\\
&-\frac{1}{2}\left[|\tau_{11}|^2 - |\tau_{02}|^2 + \mathrm{Re}(\lambda_2\tau_{21})\right],
\end{aligned} \tag{4.5}$$

$$\begin{aligned}
\tau_{20} &= \frac{1}{8}\left[F_{XX} - F_{YY} + 2G_{XY} + i(G_{XX} - G_{YY} - 2F_{XY})\right]_{(0,0)},\\
\tau_{11} &= \frac{1}{4}\left[F_{XX} + F_{YY} + i(G_{XX} + G_{YY})\right]_{(0,0)},\\
\tau_{02} &= \frac{1}{8}\left[F_{XX} - F_{YY} - 2G_{XY} + i(G_{XX} - G_{YY} + 2F_{XY})\right]_{(0,0)},\\
\tau_{21} &= \frac{1}{16}\Big\{\Big[F_{XXX} + F_{XYY} + G_{XXY} + G_{YYY}\\
&\quad + i(G_{XXX} + G_{XYY} - F_{XXY} - F_{YYY})\Big]\Big\}_{(0,0)}.
\end{aligned}$$

We now come to the following conclusion as a result of the analysis derived above.

Theorem 4.1. *Let the parameters $(a, b, c, g, h, \alpha, \rho) \in \mathbb{S}$ and δ_0 and ρ_0 be defined as in (4.1). If the parameter ρ varies in a vicinity of ρ_0 (correspondingly, δ varies around δ_0) and $L \neq 0$, then system (1.22) undergoes a Neimark–Sacker bifurcation at the fixed point point $E_3(x_3, y_3)$. Moreover, if $L < (>)0$, then a stable (an unstable) smooth closed invariant curve can be bifurcated out and the bifurcation is supercritical (subcritical).*

4.2. Period-doubling bifurcation at the fixed point E_3

From Case 3 in the proof of Theorem 3.6 for the stability of the positive fixed point E_3, one can see that the dimension numbers change for the stable manifold and unstable manifold of system (1.22) at the fixed point E_3 when δ varies in the vicinity of δ_1 (correspondingly, ρ varies in the vicinity of ρ_0) for $4B < A^2$, where

$$\delta_1 = \frac{A \pm \sqrt{A^2 - 4B}}{B}, \quad \rho_0 = \left(\Gamma(\alpha+1)\delta_1\right)^{\frac{1}{\alpha}}. \tag{4.6}$$

Hence, a bifurcation may occur. Noting that $\lambda_1 = -1$ and $|\lambda_2| \neq 1$ for $\delta = \delta_1$, we show that this bifurcation is a period-doubling one. Let

$$\begin{aligned}
S_1 = \{&(a, b, c, g, h, \alpha, \rho) \in \mathbb{R}_+^5 \ \big| \ c > g,\\
&0 < h < \frac{ag(c-g)}{c^2}, 4B < \frac{A^2}{4}\}.
\end{aligned} \tag{4.3}$$

To analyze the period-doubling bifurcation of system (1.22) at the fixed point E_3, it suffices for us to consider δ to vary in the neighborhood of $\delta_1 = \frac{A+\sqrt{A^2-B^2/4}}{B}$. The proof for the case where $\delta_1 = \frac{A-\sqrt{A^2-B^2/4}}{B}$ is completely similar and will be omitted here.

Now, proceed in the following way. Put $X_n = x_n - x_3$ and $Y_n = y_n - y_3$, which transforms the fixed point E_3 to the origin $O(0, 0)$. Consider ρ^* as a small perturbation of ρ, namely, $\rho^* = \rho - \rho_0$, with $0 < |\rho^*| \ll 1$. The perturbation takes system (1.22) into

$$\begin{cases}
X_{n+1} = X_n + \dfrac{(\rho_0+\rho_*)^\alpha}{\Gamma(\alpha+1)}\Big(\dfrac{X_n + x_3}{1 + Y_n + y_3} - (X_n + x_3)\\
\qquad + a(X_n + x_3)^2 - b(X_n + x_3)(Y_n + y_3) - h\Big),\\
Y_{n+1} = Y_n + \dfrac{(\rho_0+\rho_*)^\alpha}{\Gamma(\alpha+1)}\left(c(X_n + x_3)(Y_n + y_3) - g(Y_n + y_3)\right),\\
\rho_{n+1}^* = \rho_n^*.
\end{cases} \tag{4.7}$$

Taylor expanding of the system (4.7) at $(X, Y, \rho^*) = (0, 0, 0)$ takes the form

$$\begin{cases} X_{n+1} = a_{100}X_n + a_{010}Y_n + a_{001}\rho_n^* + a_{200}X_n^2 + a_{020}Y_n^2 \\ \quad +a_{002}\rho_n^{*2} + a_{110}X_nY_n + a_{101}X_n\rho_n^* + a_{011}Y_n\rho_n^* + a_{300}X_n^3 \\ \quad +a_{030}Y_n^3 + a_{003}\rho_n^{*3} + a_{210}X_n^2Y_n + a_{201}X_n^2\rho_n^* + a_{102}X_n\rho_n^{*2} \\ \quad +a_{120}X_nY_n^2 + a_{111}X_nY_n\rho_n^* + a_{012}X_nY_n^2 + a_{021}Y_n^2\rho_n^* + O(\rho_1^4), \\ Y_{n+1} = b_{100}X_n + b_{010}Y_n + b_{001}\rho_n^* + b_{200}X_n^2 + b_{020}Y_n^2 \\ \quad +b_{002}(\rho_n^{*2} + b_{110}X_nY_n + b_{101}X_n\delta_n^* + b_{011}Y_n\delta_n^* + b_{300}X_n^3 \\ \quad +b_{003}\rho_n^{*3} + b_{210}X_n^2Y_n + b_{201}X_n^2\rho_n^* + b_{102}X_n\rho_n^{*2} + b_{120}X_nY_n^2 \\ \quad +b_{030}Y_n^3 + b_{111}X_nY_n\rho_n^* + b_{012}X_nY_n^2 + b_{021}Y_n^2\rho_n^* + O(\rho_1^4), \\ \rho_{n+1}^* = \rho_n^*, \end{cases} \tag{4.8}$$

where $\rho_2 = \sqrt{X_n^2 + Y_n^2 + (\rho_n^*)^2}$,

$$a_{100} = 1 + \frac{\rho_0^\alpha\,(1 - (y_3+1)\,(2ax_3 - a + by_3 + 1))}{\Gamma(\alpha+1)(y_3+1)},$$

$$a_{010} = -\frac{\rho_0^\alpha\left(\frac{x_3}{(y_3+1)^2} + bx_3\right)}{\Gamma(\alpha+1)}, \quad a_{001} = 0, \quad a_{002} = 0,$$

$$a_{200} = -\frac{a\,\rho_0^\alpha}{\Gamma(\alpha+1)}, \quad a_{020} = \frac{\rho_0^\alpha\,x_3}{\Gamma(\alpha+1)(y_3+1)^3},$$

$$a_{110} = \frac{\rho_0^\alpha\left(b + \frac{1}{(y_3+1)^2}\right)}{\Gamma(\alpha+1)}, \quad a_{011} = -\frac{\alpha\,\rho_0^\alpha\left(bx_3 + \frac{x_3}{(y_3+1)^2}\right)}{\Gamma(\alpha+1)\,\rho_0},$$

$$a_{101} = -\frac{\alpha\,\rho_0^\alpha\left(2ax_3 - \frac{1}{y_3+1} - a + by_3 + 1\right)}{\Gamma(\alpha+1)\,\rho_0}, \quad a_{300} = 0,$$

$$a_{030} = -\frac{x_3\,\rho_0^\alpha}{\Gamma(\alpha+1)\,(y_3+1)^4}, \quad a_{003} = 0,$$

$$a_{111} = -\frac{\alpha\,\rho_0^\alpha\left(b + \frac{1}{(y_3+1)^2}\right)}{\Gamma(\alpha+1)\,\rho_0}. \quad a_{210} = 0,$$

$$a_{201} = -\frac{a\,\alpha\,\rho_0^\alpha}{\Gamma(\alpha+1)\,\rho_0}, \quad a_{120} = \frac{\rho_0^\alpha}{\Gamma(\alpha+1)\,(y_3+1)^3},$$

$$a_{021} = \frac{x_3\,\alpha\,\rho_0^\alpha}{\Gamma(\alpha+1)\,\rho_0\,(y_3+1)^3},$$

$$a_{012} = \frac{\rho_0^\alpha\left(bx_3 + \frac{x_3}{(y_3+1)^2}\right)\left(\frac{\alpha}{2\rho_0^2} - \frac{\alpha}{2\rho_0^2}\right)}{\Gamma(\alpha+1)},$$

$$a_{102} = \frac{\rho_0^\alpha\left(\frac{\alpha}{2\rho_0^2} - \frac{\alpha}{2\rho_0^2}\right)\left(2ax_3 - \frac{1}{y_3+1} - a + by_3 + 1\right)}{\Gamma(\alpha+1)}.$$

$$b_{100} = \frac{c\,y_3\,\rho_0^\alpha}{\Gamma(\alpha+1)}, \quad b_{010} = 1, \quad b_{001} = 0,$$

$$b_{200} = 0, \quad b_{020} = 0, \quad b_{002} = 0, \quad b_{110} = \frac{c\,\rho_0^\alpha}{\Gamma(\alpha+1)},$$

$$b_{101} = \frac{\alpha\,c\,y_3\,\rho_0^\alpha}{\Gamma(\alpha+1)\,\rho_0}, \quad b_{011} = 0, \quad b_{300} = 0, \quad b_{030} = 0,$$

$$b_{003} = 0, \quad b_{210} = 0, \quad b_{201} = 0, \quad b_{120} = 0,$$

$$b_{021} = 0, \quad b_{102} = \frac{c\,y_3\,\rho_0^\alpha\left(\frac{\alpha}{2\rho_0^2} - \frac{\alpha^2}{2\rho_0^2}\right)}{\Gamma(\alpha+1)}, \quad b_{012} = 0.$$

Let

$$T = \begin{pmatrix} a_{010} & a_{010} \\ -1 - a_{100} & \lambda_2 - a_{100} \end{pmatrix},$$

which is invertible. Now, using the transformation

$$\begin{pmatrix} X_n \\ Y_n \end{pmatrix} = T \begin{pmatrix} \tilde{u} \\ \tilde{v} \end{pmatrix},$$

system (4.8) becomes

$$\begin{cases} \tilde{u}_{n+1} = -\tilde{u}_n + M(X_n, Y_n, \rho_n^*), \\ \tilde{v}_{n+1} = \lambda_2\tilde{v}_n + N(X_n, Y_n, \rho_n^*). \end{cases} \tag{4.9}$$

System (4.9) has a center manifold $W^c(0,0,0)$ at $(0,0)$ in the neighborhood of $\rho^* = 0$, which can be deduced using the center manifold theorem and is essentially expressed as

$$W^c(0,0,0) = \{(\tilde{u}_n, \tilde{v}_n, \rho^*) \in \mathbb{R}^3 : \tilde{v}_n = \eta_1\tilde{u}_n^2 + \eta_2\tilde{u}_n\rho^* + o\left((|\tilde{u}_n| + |\rho^*|)^2\right)\},$$

where

$$\eta_1 = \frac{a_{010}\left((1+a_{100})a_{200} + b_{020}(1+a_{100})^2\right)}{1-\lambda_2^2} - \frac{(1+a_{100})(a_{110}(1+a_{100}) + a_{010}b_{110}))}{1-\lambda_2^2},$$

$$\eta_2 = \frac{(1+a_{100})(a_{011}(1+a_{100}) + a_{010}b_{011})}{a_{010}(1+\lambda_2)^2} - \frac{(1+a_{100})(a_{101} + a_{010}b_{101})}{a_{010}(1+\lambda_2)^2}.$$

So, system (4.9) restrained on the center manifold $W^c(0,0,0)$ has the form:

$$\begin{aligned} \tilde{u}_{n+1} &= -\tilde{u}_n + \theta_1\tilde{u}_n^2\rho^* + \theta_2\tilde{u}_n\rho^* + \theta_3\tilde{u}_n^2 \\ &\quad + \theta_4\tilde{u}_n(\rho^*)^2 + \theta_5\tilde{u}_n^3 + o\left((|\tilde{u}_n| + |\rho^*|)^3\right) \\ &=: Z(\tilde{u}_n, \rho^*), \end{aligned}$$

where

$$\theta_1 = \frac{\eta_2\left((\lambda_2-\eta_1)a_{200}-\eta_2 b_{200}\right)+b_{020}(1+\eta_1)^2}{1+\lambda_2} - \frac{(1+\eta_1)\left((\lambda_2-\eta_1)a_{110}-\eta_2 b_{110}\right)}{1+\lambda_2},$$

$$\theta_2 = \frac{(\lambda_2-\eta_1)a_{101}-\eta_2 b_{101}}{1+\lambda_2} + \frac{(1+\eta_1)\left((\lambda_2-\eta_1)a_{011}-\eta_2 b_{011}\right)}{\eta_2(1+\lambda_2)},$$

$$\theta_3 = \frac{(\lambda_2-a_{100})\eta_1 a_{101}-a_{010}b_{101}}{1+\lambda_2} + \frac{((\lambda_2-a_{100})a_{011}-\eta_2 b_{011})(\lambda_2-a_{100})\eta_1}{a_{010}(1+\lambda_2)^2},$$

$$\theta_4 = \frac{\eta_2((\lambda_2-a_{100})a_{110}-a_{010}b_{110})(\lambda_2-1-2a_{100})}{1+\lambda_2} + \frac{2b_{020}\eta_2(1+a_{100})(\lambda_2-a_{100})}{1+\lambda_2},$$

$$\theta_5 = \frac{2a_{010}\eta_1((\lambda_2-a_{100})a_{200}-a_{010}b_{200})}{1+\lambda_2} + \frac{\eta_2(\lambda_2-1-2a_{100})a_{210}-a_{010}b_{210}}{1+\lambda_2}.$$

In order for the period-doubling bifurcation to occur, the two determinating quantities ζ_1 and ζ_2 must both be nonzero, where

$$\zeta_1 = \left(\frac{\partial^2 Z}{\partial\tilde{u}\partial\rho}+\frac{1}{2}\frac{\partial Z}{\partial\rho^*}\frac{\partial^2 Z}{\partial\tilde{u}^2}\right)\Big|_{(0,0)},$$

$$\zeta 2 = \left(\frac{1}{6}\frac{\partial^3 Z}{\partial\tilde{u}^3}+\left(\frac{1}{2}\frac{\partial^2 Z}{\partial\tilde{u}^2}\right)^2\right)\Big|_{(0,0)}.$$

Finally, the outcome of the above analysis is summarized as follows.

Theorem 4.2. *Suppose the parameters $(a,b,c,g,h,\alpha,\rho) \in S_1$ and δ_1 and ρ_0 are defined as in (4.6). If the parameter ρ varies in a neighborhood of ρ_0 (correspondingly, δ varies around δ_1) and $\xi_1\zeta_2 \neq 0$, then system (1.22) undergoes a period-doubling bifurcation at the fixed point E_3. Furthermore, for $\zeta_2 > (<)0$, the period-two orbit that bifurcates from E_3 is stable (unstable).*

5. Numerical simulation

In this section, we perform numerical simulations for the dynamical behaviors of system (1.22) using Matlab, aiming to provide readers with a more intuitive understanding of the dynamics of system (1.22).

Firstly, fix the parameter values $\alpha = 0.6, a = 5, b = 0.8, c = 0.6, g = 0.12, h = 0.15$, and let $\rho \in (0.1, 5)$. Figure 1 shows the bifurcation diagram of system (1.22) starting from the point $(x_3, y_3) = (0.4, 0.8)$, and it is clear that system (1.22) undergoes a Neimark–Sacker bifurcation at the critical value $\rho_0 = 0.316$.

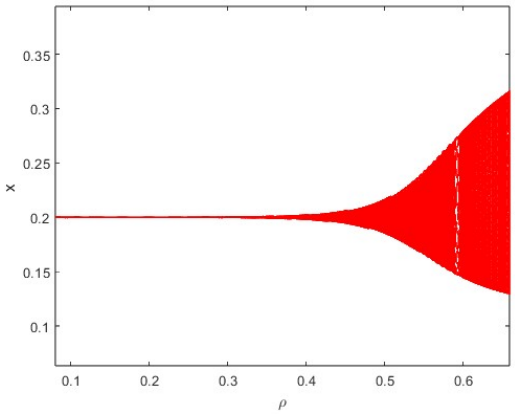

Figure 1. The existence of a Neimark–Sacker bifurcation of system (1.22) with the ρ taking values from 0.1 to 5.

With the values of $\alpha = 0.6, a = 5, b = 0.8, c = 0.08, g = 0.12$, and $h = 0.12$, Figure 2 is the bifurcation diagram of system (1.22) starting from the point $(x_3, y_3) = (0.4, 0.8)$. We can clearly observe that system (1.22) undergoes a period-doubling bifurcation at the critical value $\rho_0 = 0.2005$.

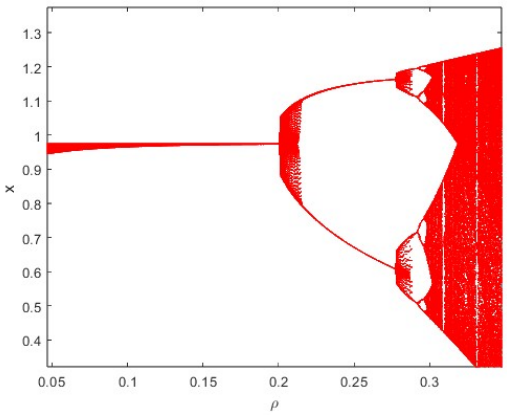

Figure 2. The existence of a period-doubling bifurcation of system (1.22) with the ρ taking values from 0.01 to 5.

Figures 3–8 depict the phase diagram of system (1.22) starting from the point $(x_0, y_0) = (0.22605, 3.25610)$ with the

parameters $\alpha = 0.6, a = 5, b = 0.8, c = 0.6, g = 0.12, h = 0.15$. We can observe that, as ρ increases, the fixed point gradually transits from stable state to unstable state, and an invariant closed curve emerges.

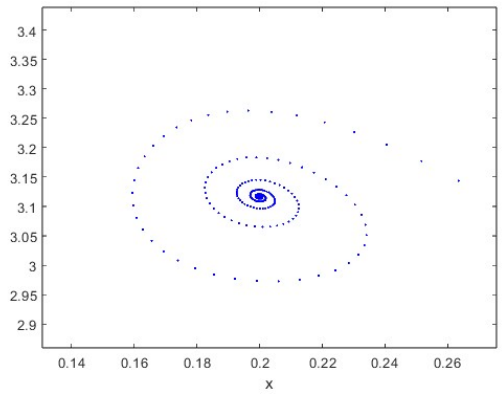

Figure 3. $\rho = 0.3$.

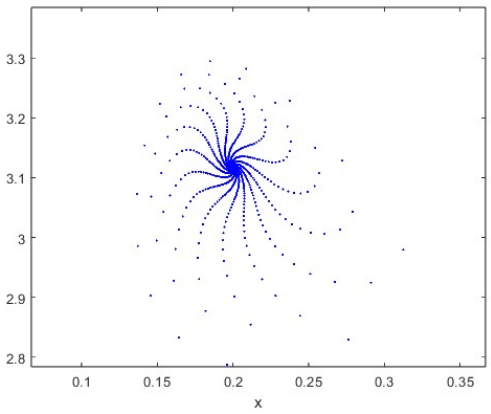

Figure 4. $\rho = 0.5$.

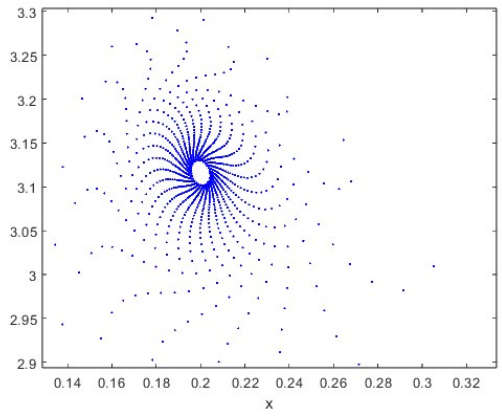

Figure 5. $\rho = 0.525$.

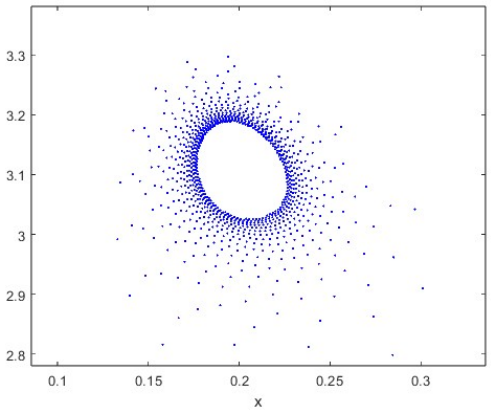

Figure 6. $\rho = 0.55$.

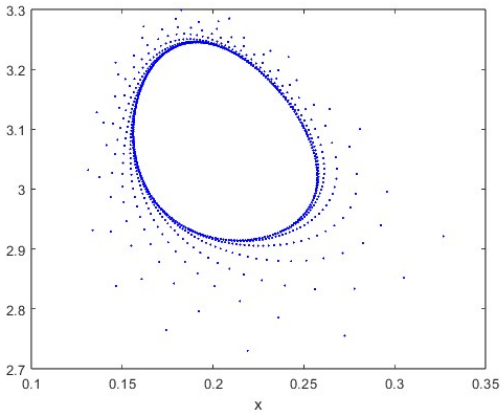

Figure 7. $\rho = 0.575$.

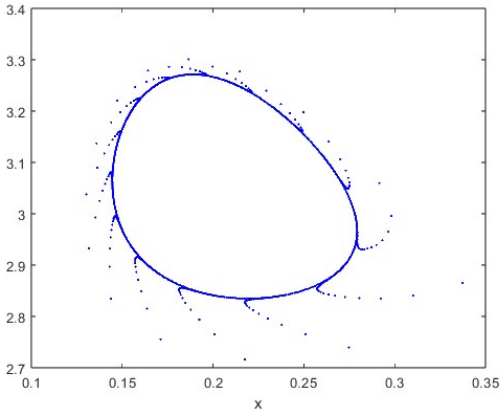

Figure 8. $\rho = 0.6$.

Figures 3–8 show system (1.22) with $\alpha = 0.6, a = 5, b = 0.8, c = 0.6, g = 0.12, h = 0.15$ and different ρ when the initial value $(x_0, y_0) = (0.22605, 3.25610)$.

6. Conclusions

In this paper, we investigate the discrete version of a fractional-order predator–prey model incorporating fear effect and constant harvesting. In system (1.1), we consider that the fear effect induced by the predator also influences the prey population. Consequently, we refine the net growth rate function of the traditional logistic model. Furthermore, by introducing a constant harvest in system (1.5), our model more accurately reflects natural dynamics. Due to the current lack of effective methods for studying the dynamics of fractional-order differential systems, we employ the piecewise constant approximation method to discretize the continuous fractional-order predator–prey system (1.22), analyze the system's dynamical properties, and discuss the types of bifurcations that may occur. Given parameter conditions, we completely formulate the existence and stability of nonnegative fixed points $E_0 = (\frac{1}{2}, 0)$, $E_1\left(\frac{1-\sqrt{1-4\frac{h}{a}}}{2}, 0\right)$, $E_2\left(\frac{1+\sqrt{1-4\frac{h}{a}}}{2}, 0\right)$ and E_3 $(\frac{g}{c}, \frac{1}{2}[\sqrt{(P+\frac{b+1}{b})^2-4P}-(\frac{b+1}{b}+P)])$ where $P = \frac{-acg+ag^2+c^2h}{bcg}$ for $c > g$ and $0 < h < \frac{ag(c-g)}{c^2}$.

We not only derive some sufficient conditions for the Neimark-Sacker bifurcation and period-doubling bifurcation to occur at the fixed points E_3 in certain parameter spaces, but also state the stability and direction of the closed bifurcated orbits. Finally, some interesting dynamical properties for Neimark-Sacker bifurcation and period-doubling bifurcation are illustrated through the application of numerical simulations.

Author contributions

All authors contributed equally and significantly in writing this paper. All authors read and approved the final manuscript.

Use of Generative-AI tools declaration

The authors declare they have not used Artificial Intelligence (AI) tools in the creation of this article.

Acknowledgments

This work is partly supported by the National Natural Science Foundation of China (61473340), the Distinguished Professor Foundation of Qianjiang Scholar in Zhejiang Province (F708108P01) and the Natural Science Foundation of Zhejiang University of Science and Technology (0401108P10).

Conflict of interest

The authors declare no conflicts of interest.

References

1. A. H. Holt, Z. G. Davies, C. Tyler, S. Staddon, Meta-analysis of the effects of predation on animal prey abundance: evidence from UK vertebrates, *PLoS ONE*, **3** (2008), e2400. https://doi.org/10.1371/journal.pone.0002400
2. R. K. Smith, A. S. Pullin, G. B. Stewart, W. J. Sutherland, Effectiveness of predator removal for enhancing bird populations, *Conserv. Biol.*, **24** (2010), 820–829. http://doi.org/10.1111/j.1523-1739.2009.01421.x
3. S. Creel, D. Christianson, Relationships between direct predation and risk effects, *Trends Ecol. Evol.*, **23** (2008), 194–201. http://doi.org/10.1016/j.tree.2007.12.004
4. W. Cresswell, Non-lethal effects of predation risk in birds, *IBIS*, **150** (2008), 3–17. http://doi.org/10.1111/j.1474-919X.2007.00793.x
5. P. A. Abrams, Foraging time optimization and interactions on food webs, *Am. Nat.*, **124** (1984), 80–96. https://doi.org/10.1086/284253
6. P. A. Abrams, Strengths of indirect effects generated by optimal foraging, *Oikos*, **62** (1991), 167–176. https://doi.org/10.2307/3545262
7. M. Haque, A detailed study of the Beddington-DeAngelis predator-prey model, *Math. Biosci.*, **234** (2011), 1–16. http://doi.org/10.1016/j.mbs.2011.07.003

8. M. T. Alves, F. M. Hilker, Hunting cooperation and Allee effects in predators, *J. Theor. Biol.*, **419** (2017), 13–22. http://doi.org/10.1016/j.jtbi.2017.02.002
9. F. Capone, M. F. Carfora, R. De Luca, I. Torcicollo, Turing patterns in a reaction-diffusion system modeling hunting cooperation, *Math. Comput. Simul.*, **165** (2019), 172–180. http://doi.org/10.1016/j.matcom.2019.03.010
10. Y. Chow, S. R. J. Jang, H. M. Wang, Cooperative hunting in a discrete predator-prey system, *J. Biol. Dyn.*, **13** (2019), 247–264. http://doi.org/10.1080/17513758.2018.1555339
11. J. Duarte, C. Januario, N. Martins, J. Sardanys, Chaos and crises in a model for cooperative hunting: a symbolic dynamics approach, *Chaos*, **19** (2009), 1–12. http://doi.org/10.1063/1.3243924
12. S. Pal, N. Pal, S. Samanta, J. Chattopadhyay, Effect of hunting cooperation and fear in a predator-prey model, *Ecol. Complex.*, **39** (2019), 1–18. http://doi.org/10.1016/j.ecocom.2019.100770
13. N. C. Pati, G. C. Layek, N. Pal, Bifurcations and organized structures in a predator-prey model with hunting cooperation, *Chaos Soliton. Fract.*, **140** (2020), 1–11. https://doi.org/10.1016/j.chaos.2020.110184
14. Z. Shang, Y. Qiao, L. Duan, J. Miao, Bifurcation analysis in a predator-prey system with an increasing functional response and constant-yield prey harvesting, *Math. Comput. Simul.*, **190** (2021), 976–1002. http://doi.org/10.1016/j.matcom.2021.06.024
15. J. Liouville, Troisième mémoire sur le développement des fonctions ou parties de fonctions en séries dont les divers termes sont assujettis à satisfaire à une même équation différentielle du second ordre, contenant un paramètre variable, *J. Math. Pures Appl.*, **2** (1837), 418–436.
16. M. Riesz, L'intégrale de riemann-liouville et le problème de cauchy pour l'équation des ondes, *Bull. Soc. Math. Fr.*, **67** (1939), 153–170. http://doi.org/10.24033/bsmf.1309
17. M. Caputo, Linear models of dissipation whose q is almost frequency independent—II, *Geophys. J. Int.*, **13** (1967), 529–539. http://doi.org/10.1111/j.1365-246X.1967.tb02303.x
18. A. A. Kilbas, H. M. Srivastava, J. J. Trujillo, Theory and applications of fractional differential equations, In: *North-Holland mathematics studies*, Vol. 24, Elsevier, 2006.
19. I. Podlubny, Fractional differential equations: an introduction to fractional derivatives, fractional differential equations, to methods of their solution and some of their applications, In: *Mathematics in science and engineering*, Elsevier, 1999.
20. A. M. A El-Sayed, Fractional-order diffusion-wave equation, *Int. J. Theor. Phys.*, **35** (1996), 311–322. http://doi.org/10.1007/bf02083817
21. H. L. Li, Y. L. Jiang, Z. L. Wang, C. Hu, Global stability problem for feedback control systems of impulsive fractional differential equations on networks, *Neurocomputing*, **161** (2015), 155–161. http://doi.org/10.1016/j.neucom.2015.02.053
22. E. Ahmed, A. S. Elgazaar, On fractional order differential equations model for nonlocal epidemics, *Phys. A: Stat. Mech. Appl.*, **379** (2007), 607–614. http://doi.org/10.1016/j.physa.2007.01.010
23. S. Das, P. K. Gupta, A mathematical model on fractional Lotka–Volterra equations, *J. Theor. Biol.*, **277** (2011), 1–6. http://doi.org/10.1016/j.jtbi.2011.01.034
24. M. Javidi, N. Nyamoradi, Dynamic analysis of a fractional order prey–predator interaction with harvesting, *Appl. Math. Model.*, **37** (2013), 8946–8956. http://doi.org/10.1016/j.apm.2013.04.024
25. F. A. Rihan, S. Lakshmanan, A. H. Hashish, R. Rakkiyappan, E. Ahmed, Fractional-order delayed predator–prey systems with Holling type-II functional response, *Nonlinear Dyn.*, **80** (2015), 777–789. http://doi.org/10.1007/s11071-015-1905-8
26. E. Ahmed, A. M. A. El-Sayed, H. A. A. El-Saka, Equilibrium points, stability and numerical solutions of fractional-order predator–prey and rabies models, *J. Math. Anal. Appl.*, **325** (2007), 542–553. http://doi.org/10.1016/j.jmaa.2006.01.087

27. S. Debnath, P. Majumdar, S. Sarkar, U. Ghosh, Memory effect on prey–predator dynamics: Exploring the role of fear effect, additional food and anti-predator behaviour of prey, *J. Comput. Sci.*, **66** (2023), 101929. http://doi.org/10.1016/j.jocs.2022.101929

28. A. Singh, V. S. Sharma, Bifurcations and chaos control in a discrete-time prey–predator model with Holling type-II functional response and prey refuge, *J. Comput. Appl. Math.*, **418** (2023), 114666. http://doi.org/10.1016/j.cam.2022.114666

29. S. Kumar, R. Kumar, C. Cattani, B. Samet, Chaotic behaviour of fractional predator-prey dynamical system, *Chaos Soliton. Fract.*, **135** (2020), 109811. https://doi.org/10.1016/j.chaos.2020.109811

30. P. Majumdar, B. Mondal, S. Debnath, U. Ghosh, Controlling of periodicity and chaos in a three dimensional prey-predator model introducing the memory effect, *Chaos Soliton. Fract.*, **164** (2022), 112585. http://doi.org/10.1016/j.chaos.2022.112585

31. A. M. Yousef, S. Z. Rida, Y. G. Gouda, A. S. Zaki, Dynamical behaviors of a fractional-order predator–prey model with Holling type IV, *Int. J. Nonlinear Sci. Numer. Simul.*, **20** (2019), 125–136. http://doi.org/10.1515/ijnsns-2017-0152

32. K. Diethelm, *The analysis of fractional differential equations. An application-oriented exposition using differential operators of Caputo type*, Lecture Notes in Mathematics, Springer, 2010. http://doi.org/10.1007/978-3-642-14574-2

33. W. Li, X. Li, Neimark–Sacker bifurcation of a semi-discrete hematopoiesis model, *J. Appl. Anal. Comput.*, **8** (2018), 1679–1693. http://doi.org/10.11948/2018.1679

AIMS Press